Phys. Chem. Glasses: Eur. J. Glass Sci. Technol. B, December 2017, **58** (6), 237–242

Indentation cracking behaviour and structures of nanophase separation of glasses

Shangcong Cheng, Chengyu Song, Peter Ercius*

National Center for Electron Microscopy, Lawrence Berkeley National Laboratory, Berkeley, CA 94720, USA

Cristian Cionea & Peter Hosemann

Department of Nuclear Engineering, University of California Berkeley, Berkeley, CA 94720, USA

Manuscript received 22 November 2016
Revised version received 6 July 2017
Accepted 28 September 2017

Correlative microscopy is used to compare the performance and nanophase structures of soda–lime–silica, fused silica and borosilicate glasses using Vickers indentation crack analysis and the transmission electron microscopy (TEM) Fresnel contrast method. It is found that the observed indentation cracking behaviour is correlated to the nanophase separation structure of these glasses. The so-called "normal" cracking behaviour of soda–lime–silica glass is influenced by its spinodal nanophase separation; while the "anomalous" cracking behaviour of fused silica is due to the uniform single phase structure. Borosilicate glass has a droplet nanophase separation and shows "intermediate" cracking behaviour. These results indicate that in order to produce low brittleness glasses it is important to control nanophase separation structure of a glass.

1. Introduction

Traditionally, glasses, as the classic brittle materials, do not experience delayed failure like ductile metals, and the catastrophic sudden advancement of cracks is predominant. The importance of fracture toughness for glasses employed in engineering applications (e.g. architectural, automobile, display and touch-screen devices) cannot be overstated.[1,2] One of the methods commonly used to evaluate the mechanical properties of glasses is the Vickers micro/nano-indentation method.[3,4] In the indentation experiments, the size of an impression, and the extent and nature of the surrounding cracks can be related to the mechanical properties of a material. According to the model developed by Yoffe, the formation of cracks during indentation is driven by tensile stresses between the plastic deformation volume below the indenter tip and the surrounding elastically deformed material. The differences in the characteristic crack patterns in glasses arise from the transition of a densification-controlled towards a shear-mediated indentation deformation.[5,6] During Vickers indentation, soda–lime–silica glass deforms to a large extent by a shearing response and forms median/radial and lateral growing cracks. However, fused silica glass deforms dominantly by densification and has a tendency to form ring and cone-like cracks, the behaviour of soda–lime–silica glass and fused silica glass are commonly considered as "normal" and "anomalous", respectively.[7,8]

Through efforts to produce glasses with higher toughness, several research groups have found new low brittleness glasses. Sehgal & Ito reported that a new formulated glass (density 2·4 g/cm^3 and chemical formulation $13Na_2O.1K_2O.4MgO.1CaO.2Al_2O_3.79SiO_2$) was less brittle compared to commercial soda–lime–silica glasses.[9,10] As shown in Figure 1, reprinted from Ref. 9, the soda–lime–silica glass under Vickers indentation at 300 gf load exhibited cracking at the four corners of the indent, whereas the new low brittleness glass exhibited no cracking. Following this discovery by Sehgal & Ito, others also found that some glasses could exhibit a so-called "intermediate" indentation response.[11–13] The intermediate glasses take on some characteristics of both normal and anomalous behaviour under the Vickers indenter. These intermediate glasses at 200 gf load not only have less median/radial cracks than soda–lime–silica glass, but also have less ring/cone

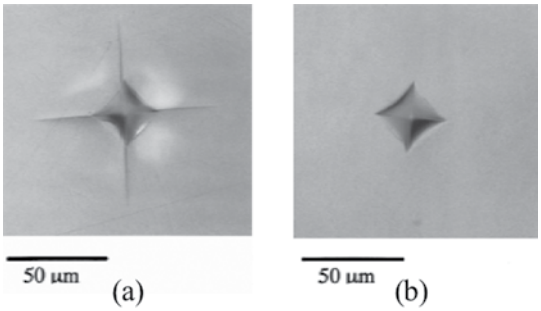

Figure 1. Vickers indentation patterns for (a) soda–lime–silica glass and (b) the new low-brittleness glass, showing the normal and anomalous cracking behaviour, respectively (Reprinted with permission from Ref. 9)

* Corresponding author. Email cheng303@gmail.com
DOI: 10.13036/17533562.58.6.040

cracks than fused silica glass. In order to understand these cracking behaviour of various glasses, several physical parameters, such as the density, Poisson's ratios and the coordination of boron in the glass have been correlated with the cracking behaviour.[10–14]

It is well known that phase structures influence certain physical and chemical properties of glasses.[15–17] It has been reported that the fracture toughness of glasses is influenced by the phase separated structure.[18–20] However, the features in the investigated structures were about μm in the size. Due to the limited spatial resolution of the TEM sample preparation method used in those previous experiments, the nanophase structures of those glasses could not be revealed. To the best of our knowledge, there are no studies correlating the indentation cracking behaviour with the structures of nanophase separation structure for glasses. A fundamental understanding of glass nanophase structure and its relationship to the cracking behaviour may provide support of research into new less brittle glasses. We compare the Vickers indentation cracking behaviour and nanophase structures for soda–lime–silica, sodium borosilicate and fused silica glasses and show a correlation between the cracking behaviour nanophase structure.

2. Experimental

2.1. Glasses

Three types of glasses were studied: soda–lime–silica, borosilicate and fused silica. Optical microscope slides (manufactured by Karter Scientific Labware Manufacturing Co., Lake Charles, USA) provided the soda–lime–silica glass sample material. The borosilicate glass source was bakeware (made by Arc International, Arques, France). Both glasses are commercially available. The fused silica glass was a Corning 7980 high purity glass containing less than 10 ppb of total metal impurities and was used before to study the optical properties of silica glass.[21]

2.2. The indentation experiments

The indentation experiments were carried out on a Tukon Microhardness Tester (Acco Wilson Instrument), with a standard diamond Vickers indenter. The glass samples were cleaned by alcohol and the surfaces were dry before testing in air. Indentation was performed on the tester using 300 gf and 500 gf peak loads. The tool was calibrated on a steel reference sample before the glass samples were tested. The indentation load was applied and removed manually. The dwell time at the peak load was 15 s. At least five indents were made for each sample at each load. The indents were imaged using an optical microscope (Axio Scope 10 from Zeiss with BF/DF and polarized light mode). Representative images of the average behaviour at each load of each sample were chosen.

2.3. TEM instruments, specimens and methods

The TEM study was carried out at National Center of Electron Microscopy (NCEM) facility of the Molecular Foundry at Lawrence Berkeley National Laboratory. The instruments used were a CM300 and a CM200 TEM (Philips, Amsterdam, Netherlands), attached with an Oxford INCA EDS detector and a Gatan Imaging Filter, having 1 nm spacial resolution and 0·9 eV energy resolutions.

TEM samples were prepared from pieces of the corresponding glass bulk material. Except for the cross-sectional specimen made from the indent of borosilicate glass, the samples were polished to a thickness of about 10 μm by mechanical polishing and dimpling. The final thinning to electron transparency was carried out using a Gatan PIPS™ ion mill. The acceleration voltage of the ion beam was 6 kV with the final thinning at 3 kV at a 7° incident angle. The specimens were coated with a thin carbon layer in a vacuum chamber to minimize charging during TEM imaging.

Because the indented regions are only at the scale of a few tens of micrometres, the cross-sectional TEM specimen from the centre of the indent made in borosilicate glass at 300 gf peak load could not be prepared by the conventional sample preparation method. Instead, it was prepared by a focused ion beam/scanning electron microscope (FIB/SEM) instrument (FEI Strata 235 dual Beam). The details of the specimen preparation by FIB/SEM can be found in the literature.[22]

The Fresnel contrast imaging method (a phase contrast technique) was used to reveal the nanophase structures of the glasses. This method was previously described in more detail.[23] Fresnel contrast images are obtained with the objective lens several microns out of focus. The image contrast depends on the difference in the inner potentials of the material phases, rather than the difference of the scattering powers. For electron radiation sensitive glass specimens, the electron dose and the area exposed to the electron beam have to be carefully monitored, so that the

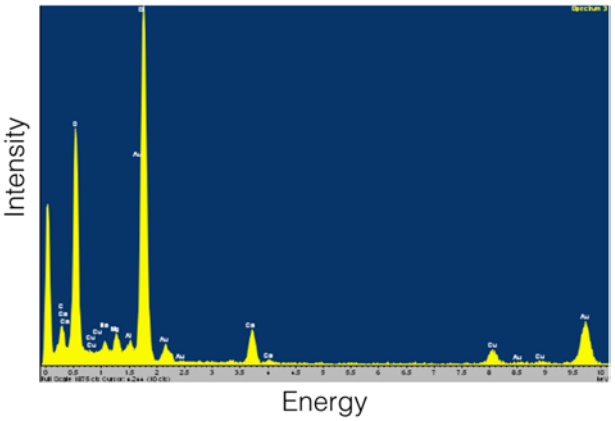

Figure 2. EDS data of the commercial soda–lime–silica glass, showing the presence of Si, O, Ca, Na, Al and Mg in the specimens. The Au and Cu signals originate from the TEM Au grid

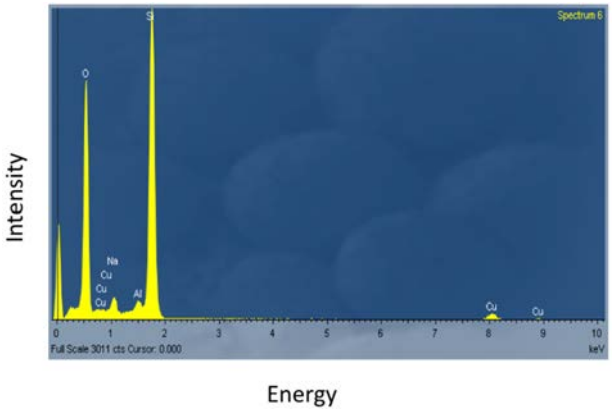

Figure 3. EDS data of the commercial borosilicate glass, showing the presence of Si, O, Na and Al in the specimen. The Cu signal originates from the TEM Cu grid, not from the specimen

nanophase structures of the glasses can be reliably observed by the Fresnel contrast images.

Energy dispersive x-ray spectroscopy (EDS) in a TEM was used to check the chemical compositions of the commercial samples. EDS was also used together with electron energy loss spectroscopy (EELS) to monitor the possible chemical and structural changes of the specimens caused by the electron beam during observation. The energy loss near edge structure (ELNES) of the boron K-edge was used to study whether or not boron coordination in the borosilicate glass was changed by the mechanical pressure of the indentation process.

3. Results

3.1. TEM results

3.1.1. Compositional analysis by EDS

The EDS data from the soda–lime–silica glass specimen in Figure 2 shows the presence of Si, O, Ca, Na, Al and Mg. The Au and Cu signals originate from the Au TEM grid. These chemical compositions are consistent with that of soda–lime–silica glass in other studies (approximate compositions, in percentages by weight: SiO_2, 72; Na_2O, 15; CaO, 5; MgO, 4; Al_2O_3, 2 and K_2O, 1).[23] Figure 3 shows the EDS data of the borosilicate glass specimen, indicating the presence of Si, O, Na and Al. The Cu signal in Figure 3 originates from the Cu TEM grid, and not from the specimen. Boron cannot be detected by this EDS system and its presence was confirmed by EELS as described in section 3.1.3. The chemical compositions of the borosilicate glass specimen are also consistent with that of previous study (approximate compositions, in percentages by weight: SiO_2, 81; B_2O_3, 13; Na_2O, 4 and Al_2O_3, 2).[23]

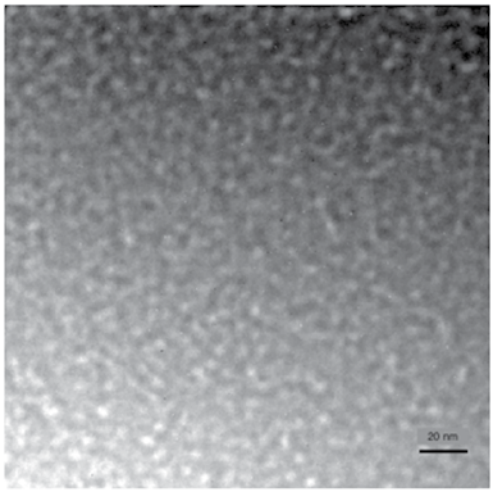

Figure 4. Fresnel contrast TEM image of the soda–lime–silica glass specimen, taken with over focus about 6 μm. The cross-section of the interpenetrating structure in the image is estimated to be 5 nm

3.1.2. Nanophase separation of glasses revealed by TEM

The soda–lime–silica glass sample is relatively unstable under the electron beam irradiation. Therefore, during the Fresnel contrast imaging process care was taken to limit the exposure, as described in previous work.[23] Figure 4 shows the Fresnel contrast TEM image (taken with over focus about 6 μm) of the soda–lime–silica glass specimen. The image indicates that soda–lime–silica glass structure exhibits a spinodal nanophase separation. The cross-section of the interpenetrating structure is estimated at around 5 nm. The nanophase structure of the soda–lime–silica glass found here is similar to that of soda–lime–silica Pyrex glass manufactured by World Kitchens LLC

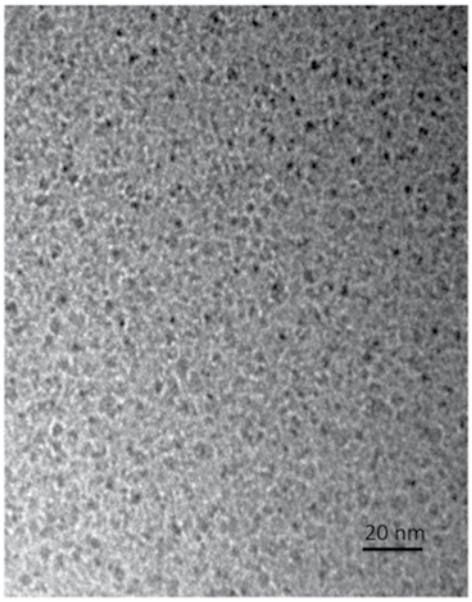

Figure 5. Fresnel contrast TEM image of the borosilicate glass specimen, taken with under focus about 2 μm. The image shows the droplet nanophase separated structure. The droplets are almost uniformly dispersed in the matrix. The average size of the droplet nanophase in the image is estimated being around 3 nm

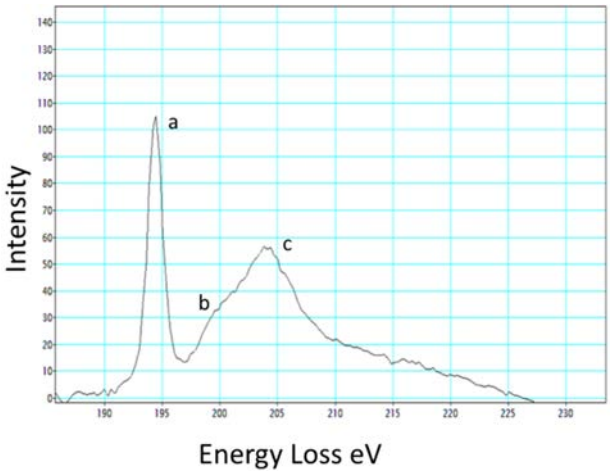

Figure 6. The ELNES of boron K-edge from borosilicate glass before the indentation. The profile of the edge indicates that the majority of B ions in the specimen have triangular coordination, and the minority have tetrahedral coordination

(Rosemont, ILL).[23] The TEM image of fused silica glass (not included) shows a uniform structure without phase separation.

The Fresnel contrast TEM image of the borosilicate glass specimen, taken with under focus about 2 μm, is shown in Figure 5. The image clearly shows a droplet nanophase separated structure. The droplets are almost uniformly dispersed in the matrix. The average diameter of the droplets is estimated at around 3 nm.

3.1.3. ELNES profile of the boron K-edge

It was suggested that the appearance of fewer indentation cracks in some boron containing glasses might be due to the change of B coordination under pressure.[24] If 3-coordinated (trigonal) B changed to 4-coordinated (tetrahedral) B under the indentation process by absorbing part of the mechanical energy, then such absorption might result in cracks with shorter lengths. To test this hypothesis, the ELNES of boron K-edge in borosilicate glass before and after indentation were analyzed and compared.

Figure 6 shows the ELNES of the boron K-edge from borosilicate glass before the indentation. No significant change of the ELNES profile was observed during electron irradiation. From literatures, oxides with planar trigonal B have features in the boron K-edge dominated by an intense sharp peak at 194 eV (peak a), called the π^* peak, followed by a broad peak with a maximum at 203 eV (peak c), called the σ^* peak. Oxides that contain only tetrahedral coordinated B have features dominated by an initial sharp rise in intensity with a maximum at 199 eV (peak b).[25] The fine structure of the boron K-edge in Figure 6 suggests that the majority of the B ions in the specimen have trigonal coordination, and the minority have tetrahedral coordination.

The SEM image in Figure 7 shows the cross-sectional specimen prepared by the FIB instrument from the centre of an indent made in borosilicate glass at the peak load of 300 gf. The specimen is about 20 μm long and 3 μm wide. The ELNES of the boron K-edge, shown as solid line in Figure 8, was taken from the FIB cross-sectional specimen of borosilicate glass after indentation at the area indicated by the arrow in Figure 7. Although the ratio of the signal to background of the spectrum in Figure 8 is lower than that in Figure 6 due to the small area of the cross-sectional specimen, the profile of ELNES shows no significant change compared to the profile in Figure 6, which is also overlaid as dashed line in Figure 8. Therefore, we can conclude that the coordination of the majority of B remained unchanged after the indentation process.

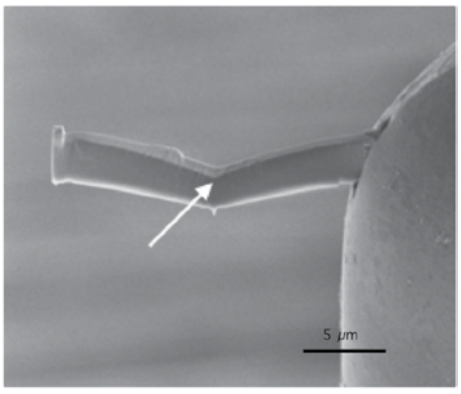

Figure 7. Scanning electron microscope (SEM) image of the cross-sectional specimen prepared by FIB instrument from the centre of an indent made in borosilicate glass at the peak load of 300 gf. The specimen is about 20 μm long and 3 μm wide. The arrow in the image points to the area right underneath the top surface of the centre of an indent

3.2. Indentation cracking results

Figures 9 and 10 show the optical images of the characteristic cracking patterns for (a) soda–lime–silica glass, (b) fused silica glass and (c) borosilicate glass,

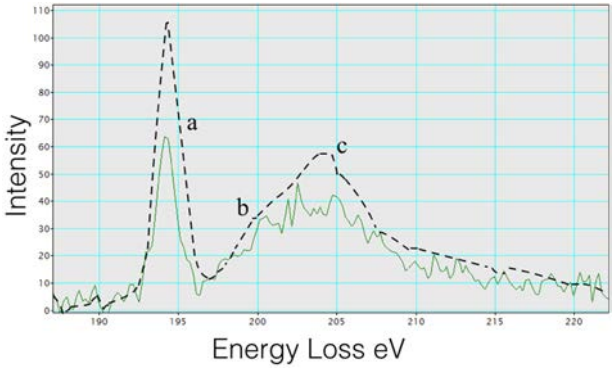

Figure 8. The ELNES of boron K-edge of borosilicate glass. Solid line was obtained from cross-sectional specimen after indentation at the area indicated by the arrow in Figure 7. The dashed line was obtained from specimen before indentation and is shown in Figure 6

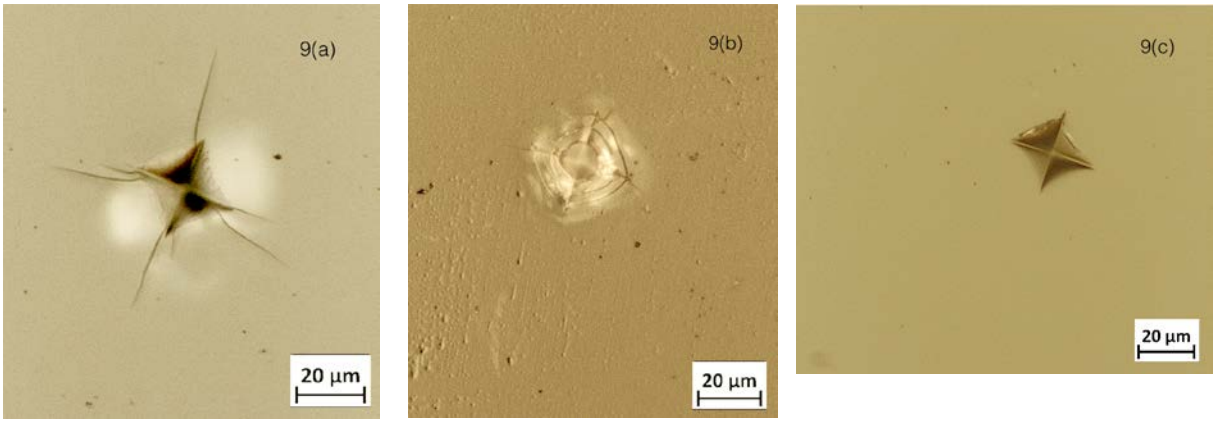

Figure 9. The optical images of the characteristic cracking patterns for (a) soda–lime–silica glass, (b) fused silica glass and (c) borosilicate glass, indented at 300 gf peak load, showing the normal, anomalous and intermediate cracking behaviour, respectively

indented at 300 gf and 500 gf peak loads, respectively. The optical images of the indentations for soda–lime–silica glass in Figures 9(a) and 10(a) show sharp, well defined median/radial cracks starting from the corners of the indent, their length increasing with the peak load. This is the "normal" cracking behaviour of soda–lime–silica glass and is in agreement with published data.[10,11]

The characteristic crack patterns around indentations in fused silica glass in Figures 9(b) and 10(b) are indicative of the "anomalous" indentation cracking behaviour. At 500 gf peak load the ring-like cracks are accompanied by radial cracks originating from indent corners. Such cracking behaviour is typical for fused silica and also consistent with that described in the literatures.[10,11]

Figures 9(c) and 10(c) show an intermediate indentation cracking behaviour of borosilicate glass that shows elements of patterns displayed by soda–lime–silicate and fused silica glasses. As compared to soda–lime–silica glass (Figure 9(a) and 10(a)), a 300 gf peak load produces no median/radial cracks in borosilicate glass (Figure 9(c)). But a 500 gf peak load (Figure 10(c)) produces sharp well-defined median/radial cracks emanating from the corners of the indent impression. However, in Figure 10(c) the crack lengths of borosilicate glass are shorter than that of soda–lime–silica glass at both 300 gf and 500 gf peak loads. As compared to fused silica glass (Figures 9(b)) a 300 gf peak load produces far fewer ring cracks in borosilicate glass (Figure 9(c)). But in Figure 10(c) at 500 gf peak load, the borosilicate glass shows defined ring cracks, similar to the anomalous cracking behaviour of fused silica glass. However, the ring cracks of the borosilicate glass in Figure 10(c) are less pronounced than those of fused silica glass at both 300 gf and 500 gf peak loads, Figures 9(b) and 10(b). Over all, the indentation cracking behaviour of borosilicate glass appears intermediate between that of soda–lime–silica glass and fused silica glass.

4. Discussions and conclusions

The results show that, similar to many other physical properties, the cracking behaviour of glasses indented with a Vickers diamond tip is correlated with their nanophase structure. Soda–lime–silica glass consists of a spinodal nanophase structure. The cracks at the corners of the indent could propagate along the relatively weaker nanophase to the outside

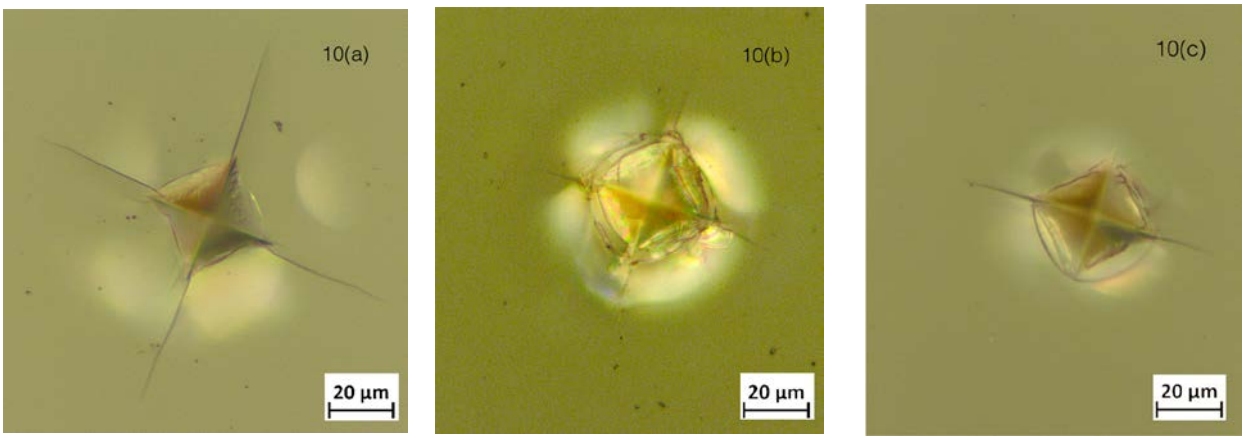

Figure 10. The same as that described in Figure 9 but indented at 500 gf peak load, showing the normal, anomalous and intermediate cracking behaviours for (a) soda–lime–silica glass, (b) fused silica glass and (c) borosilicate glass, respectively

area of the indent and allowed the formation of radial/medium cracks far from the indent. On the contrary, the single-phase structure of fused silica glass shows the so-called anomalous cracking behaviour, because there is no relatively weaker phase in the structure to provide pathways for cracks propagation. As a result, cracks in fused silica glass are more concentrated to the indented area.

For borosilicate glass, the ELNES profiles of boron K-edge suggest that the coordination of the majority of B remained unchanged after indentation. Thus, its intermediate cracking behaviour is not related to the change of B coordination during the indentation process. Borosilicate glass has a droplet nanophase separation where the relatively weaker boron rich phase is concentrated in the droplets and surrounded by a matrix phase. There is no relatively weaker phase present to form a network for crack propagation. Therefore, under the same stress condition, the lengths of the medial/radial cracks of the borosilicate glass are not as long as that of the soda–lime–silica glass. Furthermore, the amorphous droplet boron rich phase in the silica matrix might have restrained the cracks. It is well known that the strength of glass ceramics can be greatly improved by the nucleation of crystalline phase inside the glass matrix.[21] The crystalline phase in the glass matrix can restrain cracks by blunting the crack tips, or by other mechanisms.[26–28] Our experimental results indicate that the ring cracks of borosilicate glass are much less pronounced than those of fused silica due to the amorphous droplet phase. Therefore, not only the crystalline phase, but also the amorphous droplet phase in the glass matrix could restrain cracks. Many studies have shown that the size, shape and density of the crystalline phase influence the detailed cracking behaviour of glass-ceramics.[27,28] It would be expected that the cracking behaviour of the glasses with a droplet nanophase separation would also further be influenced by the size and density of the droplets.

In conclusion, the indentation cracking behaviour of glasses is found to be clearly correlated with their nanophase structures. The intermediate cracking behaviour of glasses may be related with the structure of the droplet nanophase separation. In the search for new low-brittleness glasses through changing the chemical compositions and thermal processes, it is important to also control the nanophase separation structure. Our results indicate that low-brittleness glasses will have a droplet, rather than spinodal, nanophase structure.

Acknowledgements

Work at the Molecular Foundry, Lawrence Berkeley Lab was supported by the Office of Science, Office of Basic Energy Sciences, of the US Department of Energy under Contract No. DE-AC02-05CH11231.

References

1. Wondraczek, L., Mauro, J. C., Eckert, J., Kuhn, U., Horbach, J., Deubener, J. and Rouxel, T. Towards Ultrastrong Glasses. *Adv. Mater*., 2011, **23**, 4578–4586.
2. Ellison, A. & Cornejo, I. A. Glass Substrates for Liquid Crystal Displays. *Int. J. Appl. Glass Sci*., 2010, **1**, 87–103.
3. Lawn, B. R. & Marshall, D. B. Hardness, Toughness and Brittleness: An Indentation Analysis. *J. Am. Ceram. Soc.,* 1979, **62**, 347–350.
4. Cook, R. F. & Pharr, G. M. Direct Observation and Analysis of Indentation Cracking in Glasses and Ceramics. *J. Am. Ceram. Soc.,* 1990, **73** (4), 787–817.
5. Yoffe, E. H. Elastic Stress Fields Caused by Indenting Brittle Materials. *Philos. Mag. A*, 1982, **46**, 616–628.
6. Sellappan, P., Rouxel, T., Celarie, F., Becker, E., Houizot, P. & Conradt R. Composition Dependence of Indentation Deformation and Indentation Cracking in Glass. *Acta Mater.* 2013, **61**, 5949–5965.
7. Arora, A., Marshall, D. B., Lawn, B. R., Swain, M. V. Indentation Deformation/Fracture of Normal and Anomalous Glasses. *J. Non-Cryst. Solids*, 1979, **31**, 415–428.
8. Hagan, J. T. Cone Cracks Around Vickers Indentations in Fused Silica Glass. *J. Mater. Sci.,* 1979, **14**, 462–466.
9. Sehgal, J. & Ito, S. A New Low-Brittleness Glass in the Soda-Lime Silica Glass Family. *J. Am. Ceram. Soc*., 1998, **81** (9), 2485–88.
10. Ito, S, J. Structural Study on Mechanical Behavior of Glass. *Ceram. Soc. Jpn.*, 2004, **112**, 477–485.
11. Gross, T. M. Deformation and Cracking Behavior of Glasses Indented Diamond Tips of Various Sharpness. *J. Non-Cryst. Solids*, 2012, **358**, 3445–3452.
12. Bertoldi, M. & Sglavo, V. M. Soda-Borosilicate Glass: Normal or Anomalous Behavior Under Vickers Indentation? *J. Non-Cryst. Solids,* 2004, **344**, 51–59.
13. Marina, B., Delaye, J., Charpentier, T., Gennisson, M., Bonamy, D., Rouxel, T. & Rountree, C. L. Hardness and Toughness of Sodium Borosilicate Glasses via Vicker's Indentations. *J. Non-Cryst. Solids,* 2015, **417&418**, 66–79.
14. Limbach, R., Winterstein-Beckmann, A., Dellith, J., Moncke, D. & Wondraczek, L. Plasticity, Crack Initiation and Defect Resistance in Alkali-Borosilicate Glasses: From Normal to anomalous Behavior. *J. Non-Cryst. Solids,* 2015, **417&418**, 15–27.
15. Vogel, W. *Chemistry of Glass,* The American Ceramic Society, Westerville, Ohio, 1985, P96.
16. Mazurin, O. V. & Roskova, G. P. Properties of phase-separated glasses. In *Phase separation in Glass*, Ed. O. V. Mazurin & E. A. Porai-Koshits, North-Holland 1984, P243.
17. Varshneya, A. K. *Fundamentals of Inorganic Glasses.* Society of Glass Technology, Sheffield, UK, 2006, P42, P253.
18. Miyata, N. & Jinno, H. Use of Vickers Indentation Method for Evaluation of Fracture Toughness of Phase-separated Glasses. *J. Non-Cryst. Solids*, 1980, **38&39**, 391–396.
19. Seal, A. K., Chakraborti, P., Ranjon Roy, N., Mukherjee, S., Mitra, M. K. & Das, G. C. Effect of Phase Separation on the Fracture Toughness of SiO_2-B_2O_3-Na_2O Glass. *Bull. Mater. Sci*., 2005, **5**, 457–460.
20. Haller, W. & Blackburn, D. H., Metastable Immiscibility Surface in the System Na_2O-B_2O_3-SiO_2. *J. Am. Ceram. Soc*., 1970, **53**, 34–39.
21. Cheng, S. C., Schiefelbein, S., Moore, L. L., Pierson-Stull, M., Sen, S. & Smith, C. Use of EELS to Study the Absorption Edge of Fused Silica. *J. Non-Cryst. Solids,* 2006, **352**, 3140–3146.
22. Giannuzzi, L. A. & Stevie, F. A. A Review of Focused Ion Beam Milling Techniques for TEM Specimen Preparation. *Micron*, 1999, **30**, 197–204.
23. Cheng, S., Song, C. & Ercius, P. Nanophase structures of commercial Pyrex glass cookware made from borosilicate and from soda lime silicate. *Phys. Chem. Glasses: Eur. J. Glass Sci. Technol. B*, 2015, **56** (3), 108–114.
24. Sglavo, V. M. *Lecture 9, Mechanical Properties of Glass.* http://www.certev.ufscar.br/g-cc-brasil/videos
25. Garvie, L. A. J. & Craven, A. J. Parallel Electron Energy-Loss Spectroscopy (PEELS) study of B in Minerals: The Electron Energy-Loss Structure (ELNES) of the B K edge. *Am. Miner*., 1995, **80**, 1132–1144.
26. Pannhorst, W. Glass Ceramics: State-of-the-Art. *J. Non-Cryst. Solids*, 1997, **219**, 198–204.
27. Beall, G. H. Milestones in Glass-Ceramics: a Personal Perspective. *Int. J. Appl. Glass Sci*., 2014, **5**, 93–103.
28. Wange, P., Hoche, T., Rüssel, C. & Schnapp, J. D. Microstructure-Property Relationship in High-Strength MgO-Al_2O_3-SiO_2-TiO_2 Glass-Ceramics. *J. Non-Cryst. Solids,* 2002, **298**, 137–145.